HHS Public Access

Author manuscript

*ACS Infect Dis*. Author manuscript; available in PMC 2019 December 14.

Published in final edited form as:

*ACS Infect Dis*. 2018 December 14; 4(12): 1737–1745. doi:10.1021/acsinfecdis.8b00222.

# Small Molecule Condensin Inhibitors

**Hang Zhao**[#†], **Zoya M. Petrushenko**[#†], **John K. Walker**[‡,§], **Jerome Baudry**[¶], **Helen I. Zgurskaya**[†], and **Valentin V. Rybenkov**[*,†]

[†]Department of Chemistry and Biochemistry, University of Oklahoma, 101 Stephenson Parkway, Norman, Oklahoma 73019, United States

[‡]Department of Pharmacology and Physiology, Saint Louis University School of Medicine, St. Louis, Missouri 63110, United States

[§]Department of Chemistry and Biochemistry, Saint Louis University, St. Louis, Missouri 63110, United States

[¶]Department of Biological Sciences, University of Alabama in Huntsville, 301 Sparkman Drive, Shelby Center, Huntsville, Alabama 35899, United States

[#] These authors contributed equally to this work.

## Abstract

Condensins play a unique role in orchestrating the global folding of the chromosome, an essential cellular process, and contribute to human disease and bacterial pathogenicity. As such, they represent an attractive and as yet untapped target for diverse therapeutic interventions. We describe here the discovery of small molecule inhibitors of the *Escherichia coli* condensin MukBEF. Pilot screening of a small diversity set revealed five compounds that inhibit the MukBEF pathway, two of which, Michellamine B and NSC260594, affected MukB directly. Computer-assisted docking suggested plausible binding sites for the two compounds in the hinge and head domains of MukB, and both binding sites were experimentally validated using mutational analysis and inspection of NSC260594 analogs. These results outline a strategy for the discovery of condensin inhibitors, identify druggable binding sites on the protein, and describe two small molecule inhibitors of condensins.

## Graphical abstract

[*]**Corresponding Author**, valya@ou.edu. Phone: 1(405) 325-1677. Fax: 1(405) 325-6111.

Notes

The authors declare no competing financial interest.

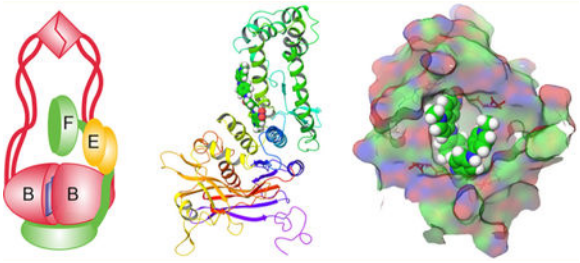


**Keywords**

condensins; MukB; HTS; novobiocin; inhibition; drug resistance

The spread of antibiotic resistant pathogens necessitates identification of novel, previously unchallenged targets and developing drugs against them.[1] Condensins represent one such new plausible target. These multisubunit partially conserved proteins are found in all kingdoms of life where they play key roles in global chromosome organization and regulate gene expression.[2–5] Condensins are essential in eukaryotic cells,[6,7] and their inactivation in bacteria leads to severe growth defects[8,9] and renders cells avirulent.[9] Thus, the development of condensin inhibitors might find diverse therapeutic applications.

The defining feature of condensins is their structure. They contain at their core a characteristically V-shaped dimer of SMC (structural chromosome maintenance) subunits.[10] The proteins act as ATP-modulated macromolecular clamps that bring distant DNA fragments together.[11] The regulatory non-SMC subunits are responsible for their intracellular recruitment and specialization.[12] Three families of condensins have been identified in bacteria, and a given species can carry one or more distinct complexes.[13] Recently, *Escherichia coli* condensins were shown to act as flux-controlling enzymes in their pathway, which qualifies them as a plausible target for inhibition.[14] However, the mechanism of condensins remains insufficiently well understood for a structure directed search for inhibitors. Similarly, the design of cell-based assays is hindered by the pleiotropic nature of condensin mutations.

We describe here a screening approach for inhibitors of the *E. coli* condensin MukBEF. The approach takes advantage of the markedly high novobiocin susceptibility of condensin deficient *E. coli*.[15] In *E. coli*, MukBEF is the sole condensin. MukB comprises the SMC core of the complex that dynamically interacts with the regulatory subunit MukEF[16,17] (Figure 1A). The novobiocin susceptibility of condensin-deficient cells resides in the two type-2 DNA topoisomerases of *E. coli*, DNA gyrase and topo IV, and presumably reflects severe deficiencies in chromosome replication and segregation of the mutants.[14,15] A physical interaction between MukBEF and topo IV has been observed *in vitro* and in vivo and shown to affect activities of both proteins.[18–21] The interaction between MukBEF and the two topoisomerases operationally defines the MukBEF pathway which might include other factors.[14]

Pilot screening of a small diversity set of 1710 compounds identified five inhibitors of the MukBEF pathway. Two of them, Michellamine B and NSC260594, were binding MukB *in*

*vitro* and induced conformational changes in the protein. The binding sites for the hits were predicted using computer assisted compound docking and then verified using site directed mutagenesis. We further tested several analogs of NSC260594 and found that they too inhibit MukB in live cells and bind it *in vitro* and that the two activities correlate with each other. Finally, we show that the found inhibitors are active against several other pathogenic bacteria.

## RESULTS

### Screening Assay for MukBEF Inhibitors.

The assay for screening employed novobiocin-dependent inhibition of growth of TolC deficient *E. coli* strain ETBW, which lacks the major outer membrane component of multidrug efflux pumps.[14] This choice of the strain helped eliminate the main source of false positives during screening. Indeed, many compounds potentiate antibiotics by improving their penetration into the cell, by either inhibiting drug efflux or disrupting the cell membrane. This is especially true for novobiocin, which happens to be an excellent substrate for multidrug efflux pumps.[22] Deletion of TolC inactivates the major multidrug transporters of *E. coli* and thereby facilitates permeation of novobiocin into the cell. Notably, multidrug efflux acts in synergy with the low permeability of the bacterial cell envelope.[23] As a result, the use of Δ*tolC* cells in the screen avoids the discovery of both membrane active drugs and inhibitors of multidrug efflux. It also increases the hit discovery rate of the screen.

After screening a library of 1710 compounds from a small diversity set from the National Cancer Institute (see Figure 1B and Materials and Methods for details), we identified nine that potentiated novobiocin (and vice versa) in Δ*tolC* cells, five of which induced phenotypes typical for Δ*mukB* cells. Chemical structures for these compounds are shown in Figure S1. These compounds were potentiated by novobiocin in *mukB*$^{+}$ ($p < 0.05$) but not Δ*mukB* cells (Figure 1C, Table S1). NSC71795 displayed the smallest potentiation, 1.4-fold, which was only barely greater than that in Δ*mukB* cells (1.2-fold), suggesting that it has the lowest specificity against the target.

Importantly, cells grown at subinhibitory concentrations of the hit compounds were impaired in the focal subcellular localization of GFP-tagged MukBEF (Figures 1D,F and S2). These cells were also deficient in chromosome partitioning and frequently produced anucleate cells (Figures 1D,E and S2). The propensity to produce clusters at the core of nucleoids is a hallmark activity of MukBEF,[12,24,25] whereas the support of chromosome segregation is its central function.[8,26] Taken together, these results indicate that the found hit compounds inhibit the MukBEF pathway. Notably, all discovered inhibitors had secondary targets inside the cell since they also decreased novobiocin-independent viability of Δ*mukB* cells (Table S1).

### Michellamine B and NSC260594 Interact with MukB *in vitro*.

We next explored interactions of the discovered hits with purified MukB using surface plasmon resonance, SPR. To this end, MukB was immobilized on the surface of a CM5 Biacore chip and 25 μM of each hit compound was injected. Two compounds, Michellamine

B (NSC661755) and NSC260594, produced a strong signal in the sensogram indicative of a strong reversible binding (Figure 2A). A much weaker binding could be detected for NSC71795 (ellipticine) and NSC45383 (streptonigrin). NSC33353 was binding the control surface, which lacked MukB, and was not pursued further.

The binding of both Michellamine B (Figure 2B) and NSC260594 (Figure 2C) was disproportionally enhanced at high concentrations of the compounds. This suggests cooperative interactions between these compounds and the protein. Accordingly, the simplest model that could be fit to the observed sensograms postulated a binding step and a conformational transition with the rate of binding allowed to increase at high concentrations of the compound (Figure 2D). Thus, the two compounds are likely to bind MukB at several sites.

### Michellamine B Inhibits MukB *in vitro*.

Chromosome organizing activity of MukB is rooted in its ability to establish bridges between distant DNA fragments.[27] To evaluate this activity, we used the magnetic bead pull down assay.[27] In this assay, MukB is loaded onto bead-tethered linear DNA, the unbound protein is removed by rinsing the beads with the reaction buffer, and another DNA is added to the beads. The beads are then rinsed again, and the captured DNA is recovered from the beads using deproteinization and quantified using gel electrophoresis. The amount of the captured DNA serves as a measure of MukB activity. We found that Michellamine B, NSC71795 and, to a smaller degree, NSC45383, inhibit MukB mediated DNA bridging, whereas no inhibition was observed for NSC260594 (Figure 3A,B). Thus, the binding of at least some of the hit compounds to MukB interferes with the biochemical activity of the protein.

We further found that Michellamine B promotes oligomerization of MukB. DNA-induced oligomerization of MukB is another activity that appears essential for its function. Owing to the oligomerization, MukB binds DNA in a highly cooperative manner, which allows it to select low occupancy DNA sites.[11] ATP-controlled oligomerization has also been reported for another bacterial condensin, SMC protein from *Bacillus subtilis*.[28] Oligomerization was detected using low speed centrifugation, through the depletion of large protein aggregates from the top half of a centrifuge tube. We found that Michellamine B but not the other hit compounds promotes oligomerization of MukB in a concentration dependent manner (Figure 3C,D). Notably, the activity appeared target specific. Among 14 tested proteins, strong oligomerization was observed only for condensins, the *E. coli* MukB and the *Pseudomonas aeruginosa* MksB (Figures 3C and S3). These data further support the notion that the binding of the hit compounds to MukB affects its activity and that the mode of interaction varies between the compounds.

### Michellamine B and NSC260594 Bind in the Hinge and the Head of MukB.

The binding sites of the hit compounds on MukB were identified using computational docking. We took advantage of the available crystal structure of the hinge domain of the *E. coli* MukB[29,30] and the head domain of *Haemophilus ducreyi* MukB.[17] We first carried out docking of Michellamine B and NSC260594 across all plausible sites on the surface of the

head and hinge domains using (i) the crystal structure of the hinge and the homology modeled head of *E. coli* MukB and (ii) hinge and head structures obtained after a 2 ns Molecular Dynamics simulation. Two preferred binding sites emerged from this docking, one at the dimer interface in the hinge and the other on the interface of the globular and coiled coil domains of the head (Figure 4A,B). Thus, the predictions of docking analysis are in full accord with the results of the experimental screen.

On the basis of the *in silico* inspection of the binding sites, we identified several residues that are predicted to interact with the hit compounds (Figure S4A,B). These residues were mutated, usually in groups, and the mutant proteins were expressed from a low copy number plasmid in Δ*mukB* cells. Immunoblotting analysis revealed that all tested proteins were expressed at similar levels (Figure S5). The resulting mutants were then assessed for novobiocin susceptibility seeking to determine whether or not the hit compounds inhibit cellular growth by directly affecting MukB. The rationale for this experiment rests on our previous finding that novobiocin susceptibility of *E. coli* gradually increases upon partial inactivation of MukBEF.[14] Therefore, novobiocin susceptibility can be used as a proxy for the remaining intracellular activity of MukBEF after its reduction by mutation or an inhibitor.

For cells expressing wild type MukB, the potentiation concentration, $PC_{50}$, of novobiocin declines as the concentration of a hit compound increases, which is consistent with a decline in the activity of MukB (Figure 4C). The concentration dependence was not the same for strains with mutant *mukB*. Two factors could be responsible for this. First, a mutated MukB could have a lower affinity to the compound, in which case more compound would be needed to achieve the same degree of MukB inhibition. Second, the mutant MukB could be less active than the wild type even in the absence of the compound, whether due to mutation or reduced expression. These two factors can be separated by relating the concentrations of the compound that yield the same $PC_{50}$ in the mutant and wild type strains (Figure 4C). As shown in Materials and Methods, the slope of the line that relates the two $PC_{50}$'s (Figure 4D) provides the low estimate for the ratio of the dissociation constants of the compound to the wild type and mutant proteins.

In these and further studies, we focused on two hit compounds, Michellamine B and NSC260594, because of their strongest effect on novobiocin potentiation (Figure 1C) and conformation of MukB (Figure 2). Most of the mutations had at least some effect on the affinity of the two compounds (Figure S4C–F). This was true for mutations in both the hinge (Figure 4E) and head (Figure 4F) domains. In general, mutations had a stronger effect on NSC260594, and some of them virtually abolished the activity of the compound. This is consistent with a relatively small size of NSC260594, which has fewer interactions with the protein than Michellamine B. Notably, all mutations that reduced the affinity of compounds to MukB were also adversely affecting its activity, which points to the functional importance of the binding site. Taken together, these data demonstrate that the cellular susceptibility to the two compounds varies depending on a mutation in MukB. We conclude, therefore, that Michellamine B and NSC260594 act by directly inhibiting MukB.

To further corroborate this conclusion, we examined whether or not cellular susceptibility to the most promising hit, NSC260594, varies depending on the expression level of MukB. To this end, we transformed Δ*tolC*Δ*mukB* cells with pBB10 plasmid, which encodes MukB under the control of an arabinose inducible promoter.[31] The cells were then grown in the presence of various amounts of arabinose and 0.1% glucose to allow graduated expression of MukB (Figure 4G). These cells were then supplemented with NSC260594, and $PC_{50}$ of novobiocin was measured. In agreement with previous studies,[14] susceptibility of cells to novobiocin declined with the increasing dosage of MukB (Figure 4H). This decline was accompanied by an increase in susceptibility to NSC260594. Thus, susceptibility of bacteria to NSC260594 can be modulated not only by mutagenesis of MukB but also by changes in its expression level.

## Structural Analogs of NSC260594 Inhibit MukB.

We next determined which structural features of the hit compounds are responsible for their activity. We focused on NSC260594, which is readily amenable to further optimization via chemical modification (Figure S1B). We found a small set of compounds at NCI with the structure related to NSC260594. We tested them for the functional and physical interaction with MukB. Compounds that contain the same core as NSC260594 (Figure 5A) were able to potentiate novobiocin (Figure 5C). Replacing the nitro group ($R_1$) with an amino group (NSC176319) led to a small improvement in activity. Similarly, switching from *N*-methyl to *N*-ethyl groups ($R_2$) at the terminal rings (NSC150517) somewhat improved the activity of the compound, whereas the addition of a nitro group to an internal phenyl ring (NSC266760) led to the 6-fold reduced activity. Curiously, we found a partially active compound, NSC67725, among distant analogs of NSC260594 (Figure 5B). This suggests that other scaffolds with anticondensin activity can be found.

To confirm that the analogs affect cellular growth via MukB, we explored their physical interaction with the protein. MukB contains eight tryptophans, which are spread throughout the molecule. Their fluorescence is quenched by the addition of NSC260594, which is indicative of a conformational transition in the protein that exposes tryptophans to a polar environment. All compounds that potentiated novobiocin demonstrated quenching of tryptophan fluorescence (Figure 5D). Unlike the other tested compounds, NSC67725 caused only partial quenching. This is consistent with the weaker effect of NSC67725 on novobiocin susceptibility and suggests a different mode of interaction of the compound with MukB. Otherwise, the apparent affinities of the compounds to MukB were consistent with their effect on novobiocin susceptibility (Figure 5D). NSC260594 had lower affinity than either NSC176319 or NSC150517 but had a higher affinity to MukB than the more distantly related analog NSC266760.

## NSC260594 and Its Analogs Have a Broad Spectrum of Activity.

Mutational inactivation of MukB increases *E. coli* susceptibility to novobiocin by more than an order of magnitude.[14,15] In principle, the same effect should be attainable through inhibition of the protein using small molecules. We indeed were able to recapitulate the phenotype of Δ*mukB* cells using sublethal concentrations of MukB inhibitors, 3/4× MIC of NSC260594 (Figure 6A) or 1/2× MIC of Michellamine B (Figure 6B). For comparison, only

little novobiocin potentiation could be observed for ciprofloxacin, which inhibits type-2 DNA topoisomerases and thereby acts in the same pathway as novobiocin, and an unrelated antibiotic rifampicin, a transcription inhibitor (Figure 6C). Thus, the ability to markedly potentiate novobiocin appears idiosyncratic to condensin inhibitors. Notably, NSC260594 potentiated nalidixic acid by about 4-fold (Figure 6D) and ciprofloxacin by 2-fold (Figure S6), indicating that condensin inhibitors can potentiate various drugs that target type-2 DNA topoisomerases.

We next evaluated the activity of NSC260594 and its more active analog NSC176319 against other bacterial pathogens. The compounds were tested against cells deficient in their permeability barrier[32] and their efflux proficient parental strains. Indeed, an efficient multidrug efflux often masks inhibition of cytoplasmic targets by bioactive compounds. The compounds displayed similar inhibition patterns, with NSC176319 being about 2-fold more active in most cases (Figure 6E, Table S2). The compounds inhibited growth of *E. coli* and *Staphylococcus aureus* at low micromolar concentrations (MIC of NSC176319 of 20 $\mu$M and 10 $\mu$M, respectively) and were also active against permeabilized *P aeruginosa* (5 $\mu$M) and *Acinetobacter baumannii* (2.5 $\mu$M; Table S2). Thus, the discovered condensin inhibitors are effective against Gram-positive and Gram-negative bacteria.

Notably, the discovered condensin inhibitors were only mildly toxic to human cells. When adherent culture of human kidney embryonic cells was grown in the presence of the inhibitors, detrimental effects on cell viability could be detected only at concentrations above 100 $\mu$M (Figure 6F). These concentrations are well above MPCs for all tested chemicals, indicating that the inhibitors have sufficient specificity for their development into antibacterial agents. Moreover, the frequency of spontaneous resistance to these compounds appeared reasonably low, less than $10^{-9}$. When $1.5 \times 10^9$ Δ*tolC E. coli* cells were plated on LB containing 8× MIC of NSC260594, no suppressors could be found (Figure S7).

## DISCUSSION

We report here the discovery of condensin inhibitors using a simple yet powerful screening approach that can be expanded to a high throughput format. Previous screening campaigns for potentiators of topoisomerase inhibitors, novobiocin and fluoroquinolones, employed efflux proficient bacteria and, as a result, identified inhibitors of multidrug efflux and cell envelope biosynthesis.[33,34] The use of efflux deficient cells helped avoid such compounds and revealed intracellular targets of novobiocin potentiators. About half of such compounds proved to be related to the MukBEF pathway, and two of them affected MukB directly. This strategy also ensured a high hit discovery rate, because most of the compounds in screening libraries either are substrates of efflux or fail to penetrate across the outer membrane of Gram-negative bacteria.[35] After screening only 1710 compounds, we identified two MukB inhibitors. Until now, only one compound capable of inhibiting condensins has been described. A quinazoline derivative Q15 was found by screening anticancer actives for interaction with human condensin II and was postulated to act via its non-SMC subunit.[36]

Notably, the compounds discovered in this study are active against diverse pathogens including Gram-positive and -negative bacteria (Figure 6E), whereas their toxicity to human

cells appears rather mild (Figure 6F). Thus, rational drug discovery against new targets can complement the ongoing efforts to repurpose existing drugs for antibacterial therapies.[37]

The discovery of MukB inhibitors demonstrates that condensins can be inhibited by small molecules and reveals the sites on the protein that are vulnerable to such inhibition. This opens up the road for structure-based drug discovery against the proteins of this class. The found druggable sites are located at two conspicuous locations, at the interface of the coiled coil and globular domains of MukB head and at the dimer interface of the hinge. These two locations are argued to be important in various mechanistic models of condensins and condensin-like proteins.[3,38] Elucidating the mechanism of inhibition by these compounds should help deduce the mechanism of MukB. A preliminary survey of MukB activities revealed that the two primary hits differ in their effect on the protein. Both compounds disrupted the activity of MukB *in vivo* (Figure 1) and were binding MukB in a SPR assay (Figure 2). However, only Michellamine B but not NSC260594 interfered with DNA binding and induced formation of large MukB aggregates (Figure 3). Clearly, the mechanism of the two compounds is not the same, most likely due to their different poses within the binding site on the protein.

Notably, the potency of NSC260594 increased with increasing concentrations of the target (Figure 4H). The opposite would be expected if the compound simply inactivated MukB thereby reducing its residual activity. Instead, the observed pattern suggests that NSC260594 might be trapping MukB in a conformation that is toxic to the cell. Indeed, an increase in the concentration of a toxic Cabundance of DNA cleavage intermediates lead to dose-dependent cellular death.[39] Similarly, antibiotics that convert ClpP into a nonspecific protease are active only in the presence of ClpP but not its absence.[40]

The discovered inhibitors offer ample opportunity for optimization. NSC176319, also known as Cain's quinolinium, is cytotoxic to leukemia and bone marrow progenitor cells[41] presumably through inhibition of DNA cytosine methyltransferase DNMT1.[42] A series of NSC176319 analogs has been recently described that displays a variable activity against DNMT1.[43] Michellamine B is a plant alkaloid shown to inhibit HIV-induced cell killing.[44] It has an interesting dimeric structure, and its stereoselective synthesis has been previously described.[45] Thus, a synthetic strategy can be readily developed for optimization of either of the two primary hits.

Molecular modeling experiments suggest the compounds bind to the target mostly through hydrophobic interactions, though a couple of electrostatic interactions are suggested. This suggests that there is room for modifications that establish additional hydrogen bonds to the target to potentially increase both the affinity and specificity of interaction. Likewise, the permeability of the compounds could be improved using medicinal chemistry methods.

## MATERIALS AND METHODS

### Plasmids and Strains.

The strains used in this study are listed in Table S3. OU151 (MG1655 Δ*mukB::kan lacYA::-mukB-gf p-spc* Δ*tolC*::*cam*) was constructed by P1*vir* transduction of the Δ*tolC::cam*

fragment from *E. coli* strain RAM1130[46] into OU116.[47] OU152 (MG1655 Δ*mukEF::kan lacYA::mukB-gf p-spc*) was constructed by P1*vir* transduction of Δ*mukEF::kan* into OU115.[47] Point mutations (summarized in Table S4) were introduced into *mukB* using PCR-assisted cloning, and the protein was expressed from a low copy number plasmid p15sp-B02a.[47] MukB dosage was varied using pBB10 plasmid, which expresses MukB-His10 from an arabinose inducible promoter.[31]

## Compound Screening.

The screened library consisted of 1593 compounds from the NCI Diversity Set V and 117 compounds of NCI Natural Products Set. The assay detected inhibition of bacterial growth by test compounds in the presence of novobiocin. $10^4$ exponentially growing Δ*tolC* ETBW cells were inoculated into each well of a microplate containing LB, 10 μM compound, 1% DMSO, and 1/4× MIC of novobiocin (0.4 μM), incubated with shaking for 16 h at 37 °C and then assessed for cellular growth by measuring light absorbance at 600 nm ($OD_{600}$). At 1/4× MIC, novobiocin concentration is high enough to allow a high hit discovery rate and, at the same time, sufficiently low to accommodate the relatively low, about 2-fold, accuracy of MIC measurements. This concentration is also well above the MIC of Δ*tolC*Δ*mukB* cells, 0.1 μM. Cell inoculations without any compound were used as a negative control whereas growth medium without bacteria were used as a positive control. The Z′-factor was typically above 0.8. Growth inhibition was called when $OD_{600}$ in a given well was below the plate average minus three standard deviations. The screen actives were then serially diluted and assessed for growth inhibition in the presence but not absence of novobiocin. All nine hits tested negative in novobiocin potentiation in Δ*tolC*Δ*mukB* OU142 cells.

## Microscopy.

Fluorescence microscopy was done as previously described.[12] Exponential cells were transferred into fresh medium, supplemented with the indicated compounds and incubated with aeration in LB for 16 h. Fifteen μL of the cells was then spotted atop of a 1% agarose pad and observed. For DNA staining in live cells, the cells were incubated with 5 μM Hoechst 33342 for 15 min. Anucleate cells were scored following fixation in 70% ethanol and staining with 100 nM DAPI and 1× Sypro Orange.

## Biochemical Assays.

Purification of *E. coli* MukB, wheat germ topoisomerase I, *P. aeruginosa* MksB, and *E. coli* membrane fusion protein AcrA has been previously described.[13,31,48] *E. coli* HNS, lac repressor LacI, the dimeric LacI,[49] dLacI, and ribosomal proteins S4 and L17 were purified using conventional chromatography resulting in 95% pure proteins. Bovine serum albumin, BSA, calf thymus thyroglobulin, carbonic anhydrase, alcohol dehydrogenase, and β-amylase were purchased from Sigma-Aldrich (MWGF1000–1KT).

DNA bridging was assessed using a magnetic bead pull down assay as previously described[50] in a reaction buffer containing 20 mM HEPES, pH 7.7, 50 mM NaCl, 2 mM $MgCl_2$, 5% glycerol, and 1 mM DTT and the indicated compounds.

For the protein aggregation assay, 2 μg of protein was incubated for 10 min at 23 °C in 25 μL of reaction buffer supplemented with compounds and then fractionated by low speed centrifugation as described in ref 50.

Tryptophan fluorescence was observed using a Shimadzu RF-5301PC spectrofluorimeter, excitation wavelength of 280 nm, emission at 336 nm, 1 × 4 × 0.1 cm cuvette. 0.1 μM MukB was dialyzed into the reaction buffer (20 mM HEPES, pH 7.0, 50 mM NaCl, 0.5% DMSO) while the compounds were diluted into the same buffer. Equal volumes of the compound and a 2-fold concentrated stock of MukB were then added to the protein to keep its concentration constant while gradually increasing the compound concentration. The tested compounds did not show any fluorescence at 336 nm but some absorbed light in this range. The observed fluorescence, $F_{obs}$, was corrected for the absorbance of the compound using the equation:

$$F = F_{obs}\frac{\log(10) \times \varepsilon c l}{1 - 10^{-\varepsilon c l}} \quad (1)$$

where $\varepsilon$ is the extinction coefficient of the compound at 336 nm, $c$ is its concentration, and $l$ is the length of the cuvette. The data were then fitted to a Langmuir dissociation curve to determine the apparent dissociation constant $K_D$.

### Surface Plasmon Resonance.

SPR studies were performed using a Biacore 3000 analyzer. Biacore CM5 chips were activated using *N*-hydroxysuccinimide (NHS) and *N*-ethyl-*N*- (3-diethylaminopropyl) carbodiimide (EDC) according to manufacturer's instructions, and 60 μg/mL MukB in 10 mM NaOAc, pH 4.0, was injected for 10 min at 10 μL/min. Cross-linking was quenched by the injection of 0.5 M ethanolamine, pH 8.0 for 5 min at 10 μL/min. Binding experiments were carried out in the buffer containing 20 mM HEPES-KOH, pH 7.0, 50 mM NaCl, 0.5% DMSO, and the indicated compounds. When needed, the chip was regenerated using 10 mM CHAPS, 20 mM HEPES, pH 7.0, 50 mM NaCl, 0.5% DMSO. The sensograms were normalized to the signal collected from a control surface, which was processed identical to the other surfaces but in the absence of any protein. The resulting binding curves were analyzed using home written scripts in MATLAB.

### Molecular Docking, Virtual Screening, and Molecular Dynamics Simulations.

The head domain of *E. coli* MukB was homology modeled on the basis of the structure of MukB from *Haemophilus ducreyi*[17] using Phyre2.[51] The program MOE (Chemical Computing Group Ltd., Montreal, Canada) version 2016 was used to perform the docking and virtual screening calculations. The protein target structures were protonated using the Protonate3D facility in MOE. The MMFF force field was used to assign protein atomic charges. Compounds were docked in the protein structures using the DOCK facility in MOE and ranked according to their predicted binding free energies calculated from the GB/WSA $\Delta G$ binding score as implemented in MOE. To release structural changes induced by crystal packing, the crystal structures were also subjected to a 2 ns Molecular Dynamics simulation, using the MOE program and the Amber99 force field and implicit solvation. For the head,

the docking results suggested the same potential binding site (shown in Figure 4) in both the crystal structure and the Molecular Dynamics structure. For the hinge, two different sites, both at the dimer interface, were identified for the crystal structure and the Molecular Dynamics structure. Docking using the Schrodinger Glide facility concurred on the binding site identified by MOE on the Molecular Dynamics structure, and it is the site (shown on Figure 4) that was subsequently validated using side directed mutagenesis.

## Novobiocin Susceptibility and Interaction.

Novobiocin susceptibility in the presence of various compounds was determined on the basis of the 2-fold serial dilution method. 10 000 exponential cells grown in LB at 37 °C (for *mukB*$^+$ cells) or 23 °C (for Δ*mukB* cells) were added into each well of a microtiter plate and supplemented with 1% DMSO, test compounds, serially diluted novobiocin and, when appropriate, 0.1% glucose and the indicated amount of arabinose. The plates were covered with AeraSeal microporous tape and a lid and incubated at 37 °C, 180 rpm for 16 h (*mukB*$^+$ cells) or 23 °C for 48 h (Δ*mukB* cells), after which their $OD_{600}$ was measured using a Tecan Spark 10 M microplate reader. The growth curves were then fit to a Hill equation to determine the half-maximal inhibitory ($IC_{50}$) or potentiation ($PC_{50}$) concentration, as appropriate.

Novobiocin susceptibility of strains with mutant MukB was measured using OU142 (Δ*tolC* Δ*mukB*) cells that harbor p15sp-B02a-X plasmids, where 'X' denotes the mutation. To compare susceptibilities of the mutants to the hit compounds, we first matched the concentrations of compounds that yield the same novobiocin susceptibility in the mutant and wild type strains as outlined in Figure 4C. We assumed that the concentrations of active MukB are the same in the two strains at these conditions. We then modeled the interaction between the compound and MukB as a 1:1 binding reaction. Given that, the uninhibited activity of MukB would follow the equation

$$A = A_{\mathrm{W}} \times \frac{K_{\mathrm{W}}}{K_{\mathrm{W}} + c_{\mathrm{W}}} = A_{\mathrm{m}} \times \frac{K_{\mathrm{m}}}{K_{\mathrm{m}} + c_{\mathrm{m}}} \quad (2)$$

where $A_{\mathrm{w}}$ and $A_{\mathrm{m}}$ are the activities of the wild type and mutant MukB, respectively, in the absence of the compound, $K_{\mathrm{w}}$ and $K_{\mathrm{m}}$ are the dissociation constants for the interaction, and $c_{\mathrm{w}}$ and $c_{\mathrm{m}}$ are the concentrations of the compound that yield the same novobiocin susceptibility in the two strains. Equation 2 can be rearranged to the following form

$$c_{\mathrm{W}} = K_{\mathrm{W}}\left(\frac{A_{\mathrm{W}}}{A_{\mathrm{m}}} - 1\right) + \frac{A_{\mathrm{W}}K_{\mathrm{W}}}{A_{\mathrm{m}}K_{\mathrm{m}}} \times c_{\mathrm{m}} \quad (3)$$

This equation describes a linear relationship between $c_{\mathrm{w}}$ and $c_{\mathrm{m}}$ with the slope of the line $a = (A_{\mathrm{w}}/A_{\mathrm{m}}) \times (K_{\mathrm{w}}/K_{\mathrm{m}})$. For all tested mutants (Figure S4), the slope of the line was less than 1 and $A_{\mathrm{w}} \geq A_{\mathrm{m}}$. Therefore, the relative affinity of the compound to the mutant MukB is $(K_{\mathrm{w}}/K_{\mathrm{m}}) = \mathrm{a} \times (A_{\mathrm{m}}/A_{\mathrm{w}}) \leq a < 1$.

### Cytotoxicity Assay.

Cytotoxicity of the compounds was evaluated using the CellTiter AQueous One Solution Cell Proliferation Assay (MTS; Promega) as previously described.[52] HEK293 cells (ATCC CRL-1573) were incubated in Eagle's Minimum Essential Medium (EMEM) (ATCC 30-2003) containing 10% fetal bovine serum (FBS) (ATCC 30-2020) at 37 °C in the presence of 5% $CO_2$. When appropriate, 20 000 cells in 80 μL of medium were seeded into Corning 96 well white polystyrene microplates with clear, tissue culture-treated flat bottoms (Corning 3903). After 24 h, compounds of interest were serially diluted and added to the cells, and DMSO was adjusted to 0.5% in the total volume of 100 μL. The cells were further incubated for 24 h at 37 °C with 5% $CO_2$. The following day, 20 μL of CellTiter AQueous One Solution Reagent was added to each well, and the cells were incubated for 4 h at 37 °C; the absorbance at 490 nm was recorded using a Tecan Spark 10 M plate reader. All measurements were done in three replicas.

## Supplementary Material

Refer to Web version on PubMed Central for supplementary material.

## ACKNOWLEDGMENTS

This work was supported in parts by the awards for the project number HR14-042 from Oklahoma Center for Advancement of Science and Technology to V.V.R., the National Institutes of Allergy and Infectious Diseases AI136799 to V.V.R. and H.I.Z. and AI052293 to H.I.Z., and HDTRA1-14-1-0019 from the Department of the Defense, Defense Threat Reduction Agency to H.I.Z. The content of the information does not necessarily reflect the position or the policy of the federal government, and no official endorsement should be inferred. The authors acknowledge the support from the National Cancer Institute (NCI)/Division of Cancer Treatment and Diagnosis (DCTD)/Developmental Therapeutics Program (DTP), http://dtp.cancer.gov.

## REFERENCES

(1). Silver LL (2016) A gestalt approach to Gram-negative entry. Bioorg. Med. Chem 24, 6379–6389. [PubMed: 27381365]

(2). Reyes-Lamothe R, Nicolas E, and Sherratt DJ (2012) Chromosome replication and segregation in bacteria. Annu. Rev. Genet 46, 121–143. [PubMed: 22934648]

(3). Rybenkov VV, Herrera V, Petrushenko ZM, and Zhao H (2015) MukBEF, a chromosomal organizer. J. Mol. Microbiol Biotechnol 24, 371–383.

(4). Hirano T (2012) Condensins: Universal organizers of chromosomes with diverse functions. Genes Dev 26, 1659–1678. [PubMed: 22855829]

(5). Cobbe N, and Heck MM (2004) The evolution of SMC proteins: Phylogenetic analysis and structural implications. Mol. Biol. Evol 21, 332–347. [PubMed: 14660695]

(6). Strunnikov AV, Hogan E, and Koshland D (1995) Smc2, a Saccharomyces-cerevisiae gene essential for chromosome segregation and condensation, defines a subgroup within the SMC family. Genes Dev 9, 587–599. [PubMed: 7698648]

(7). Hirano T, and Mitchison TJ (1994) A heterodimeric coiled-coil protein required for mitotic chromosome condensation in vitro. Cell 79, 449–458. [PubMed: 7954811]

(8). Niki H, Jaffe A, Imamura R, Ogura T, and Hiraga S (1991) The new gene mukB codes for a 177 kd protein with coiled-coil domains involved in chromosome partitioning of E. coli. EMBO J 10, 183–193. [PubMed: 1989883]

(9). Zhao H, Clevenger AL, Ritchey JW, Zgurskaya HI, and Rybenkov VV (2016) Pseudomonas aeruginosa condensins support opposite differentiation states. J. Bacteriol 198, 2936–2944. [PubMed: 27528506]

(10). Melby TE, Ciampaglio CN, Briscoe G, and Erickson HP (1998) The symmetrical structure of structural maintenance of chromosomes (SMC) and MukB proteins: Long, antiparallel coiled coils, folded at a flexible hinge. J. Cell Biol 142, 1595–1604. [PubMed: 9744887]

(11). Cui Y, Petrushenko ZM, and Rybenkov VV (2008) MukB acts as a macromolecular clamp in DNA condensation. Nat. Struct. Mol. Biol 15, 411–418. [PubMed: 18376412]

(12). She W, Mordukhova E, Zhao H, Petrushenko ZM, and Rybenkov VV (2013) Mutational analysis of MukE reveals its role in focal subcellular localization of MukBEF. Mol. Microbiol 87, 539–552. [PubMed: 23171168]

(13). Petrushenko ZM, She W, and Rybenkov VV (2011) A new family of bacterial condensins. Mol. Microbiol 81, 881–896. [PubMed: 21752107]

(14). Petrushenko ZM, Zhao H, Zgurskaya HI, and Rybenkov VV (2016) Novobiocin susceptibility of MukBEF-deficient Escherichia coli is combinatorial with efflux and resides in DNA topoisomerases. Antimicrob. Agents Chemother 60, 2949–2953. [PubMed: 26926630]

(15). Adachi S, and Hiraga S (2003) Mutants suppressing novobiocin hypersensitivity of a mukB null mutation. J. Bacteriol 185, 3690–3695. [PubMed: 12813060]

(16). Petrushenko ZM, Lai CH, and Rybenkov VV (2006) Antagonistic interactions of kleisins and DNA with bacterial condensin MukB. J. Biol. Chem 281, 34208–34217. [PubMed: 16982609]

(17). Woo JS, Lim JH, Shin HC, Suh MK, Ku B, Lee KH, Joo K, Robinson H, Lee J, Park SY, Ha NC, and Oh BH (2009) Structural studies of a bacterial condensin complex reveal ATP-dependent disruption of intersubunit interactions. Cell 136, 85–96. [PubMed: 19135891]

(18). Li Y, Stewart NK, Berger AJ, Vos S, Schoeffler AJ, Berger JM, Chait BT, and Oakley MG (2010) Escherichia coli condensin MukB stimulates topoisomerase IV activity by a direct physical interaction. Proc. Natl. Acad. Sci. U. S. A 107, 18832–18837. [PubMed: 20921377]

(19). Hayama R, and Marians KJ (2010) Physical and functional interaction between the condensin MukB and the decatenase topoisomerase IV in Escherichia coli. Proc. Natl. Acad. Sci. U. S. A 107, 18826–18831. [PubMed: 20696938]

(20). Zawadzki P, Stracy M, Ginda K, Zawadzka K, Lesterlin C, Kapanidis AN, and Sherratt DJ (2015) The localization and action of topoisomerase IV in Escherichia coli chromosome segregation is coordinated by the SMC complex, MukBEF. Cell Rep 13, 2587–2596. [PubMed: 26686641]

(21). Kumar R, Grosbart M, Nurse P, Bahng S, Wyman CL, and Marians KJ (2017) The bacterial condensin MukB compacts DNA by sequestering supercoils and stabilizing topologically isolated loops. J. Biol. Chem 292, 16904–16920. [PubMed: 28842486]

(22). Tikhonova EB, Wang Q, and Zgurskaya HI (2002) Chimeric analysis of the multicomponent multidrug efflux transporters from Gram-negative bacteria. J. Bacteriol 184, 6499–6507. [PubMed: 12426337]

(23). Westfall DA, Krishnamoorthy G, Wolloscheck D, Sarkar R, Zgurskaya HI, and Rybenkov VV (2017) Bifurcation kinetics of drug uptake by gram-negative bacteria. PLoS One 12, e0184671. [PubMed: 28926596]

(24). Shin HC, Lim JH, Woo JS, and Oh BH (2009) Focal localization of MukBEF condensin on the chromosome requires the flexible linker region of MukF. FEBS J 276, 5101–5110. [PubMed: 19674109]

(25). Ohsumi K, Yamazoe M, and Hiraga S (2001) Different localization of SeqA-bound nascent DNA clusters and MukF-MukE-MukB complex in Escherichia coli cells. Mol. Microbiol 40, 835–845. [PubMed: 11401691]

(26). Wang Q, Mordukhova EA, Edwards AL, and Rybenkov VV (2006) Chromosome condensation in the absence of the non-SMC subunits of MukBEF. J. Bacteriol 188, 4431–4441. [PubMed: 16740950]

(27). Petrushenko ZM, Cui Y, She W, and Rybenkov VV (2010) Mechanics of DNA bridging by bacterial condensin MukBEF in vitro and in singulo. EMBO J 29, 1126–1135. [PubMed: 20075860]

(28). Hirano M, and Hirano T (2004) Positive and negative regulation of SMC-DNA interactions by ATP and accessory proteins. EMBO J 23, 2664–2673. [PubMed: 15175656]

(29). Ku B, Lim JH, Shin HC, Shin SY, and Oh BH (2010) Crystal structure of the MukB hinge domain with coiled-coil stretches and its functional implications. Proteins: Struct., Funct., Genet 78, 1483–1490. [PubMed: 20034111]

(30). Li Y, Schoeffler AJ, Berger JM, and Oakley MG (2010) The crystal structure of the hinge domain of the Escherichia coli structural maintenance of chromosomes protein MukB. J. Mol. Biol 395, 11–19. [PubMed: 19853611]

(31). Petrushenko ZM, Lai CH, Rai R, and Rybenkov VV (2006) DNA reshaping by MukB. Right-handed knotting, left-handed supercoiling. J. Biol. Chem 281, 4606–4615. [PubMed: 16368697]

(32). Krishnamoorthy G, Leus IV, Weeks JW, Wolloscheck D, Rybenkov VV, and Zgurskaya HI (2017) Synergy between active efflux and outer membrane diffusion defines rules of antibiotic permeation into Gram-negative bacteria. mBio 8, e01172–17. [PubMed: 29089426]

(33). Renau TE, Leger R, Flamme EM, Sangalang J, She MW, Yen R, Gannon CL, Griffith D, Chamberland S, Lomovskaya O, Hecker SJ, Lee VJ, Ohta T, and Nakayama K (1999) Inhibitors of efflux pumps in Pseudomonas aeruginosa potentiate the activity of the fluoroquinolone antibacterial levofloxacin. J. Med. Chem 42, 4928–4931. [PubMed: 10585202]

(34). Taylor PL, Rossi L, De Pascale G, and Wright GD (2012) A forward chemical screen identifies antibiotic adjuvants in Escherichia coli. ACS Chem. Biol 7, 1547–1555. [PubMed: 22698393]

(35). Silver LL (2011) Challenges of antibacterial discovery. Clin Microbiol Rev 24, 71–109. [PubMed: 21233508]

(36). Shiheido H, Naito Y, Kimura H, Genma H, Takashima H, Tokunaga M, Ono T, Hirano T, Du W, Yamada T, Doi N, Iijima S, Hattori Y, and Yanagawa H (2012) An anilinoquinazoline derivative inhibits tumor growth through interaction with hCAP-G2, a subunit of Condensin II. PLoS One 7, e44889. [PubMed: 23028663]

(37). Tharmalingam N, Port J, Castillo D, and Mylonakis E (2018) Repurposing the anthelmintic drug niclosamide to combat Helicobacter pylori. Sci. Rep 8, 3701. [PubMed: 29487357]

(38). Williams GJ, Williams RS, Williams JS, Moncalian G, Arvai AS, Limbo O, Guenther G, SilDas S, Hammel M, Russell P, and Tainer JA (2011) ABC ATPase signature helices in Rad50 link nucleotide state to Mre11 interface for DNA repair. Nat. Struct. Mol. Biol 18, 423–431. [PubMed: 21441914]

(39). Cheng B, Shukla S, Vasunilashorn S, Mukhopadhyay S, and Tse-Dinh Y-C (2005) Bacterial cell killing mediated by topoisomerase I DNA cleavage activity. J. Biol. Chem 280, 38489–38495. [PubMed: 16159875]

(40). Conlon BP, Nakayasu ES, Fleck LE, LaFleur MD, Isabella VM, Coleman K, Leonard SN, Smith RD, Adkins JN, and Lewis K (2013) Activated ClpP kills persisters and eradicates a chronic biofilm infection. Nature 503, 365–370. [PubMed: 24226776]

(41). Naujokaitis SA (1981) Cain's quinolinium (NSC 176319): Protection of murine L1210 leukemia cells and bone marrow progenitor cells against mechlorethamine cytotoxicity and its application to combination chemotherapy. Res. Commun. Chem. Pathol. Pharmacol 34, 97–104. [PubMed: 7313308]

(42). Villar-Garea A, Fraga MF, Espada J, and Esteller M (2003) Procaine is a DNA-demethylating agent with growth-inhibitory effects in human cancer cells. Cancer Res 63, 4984–4989. [PubMed: 12941824]

(43). Gamage SA, Brooke DG, Redkar S, Datta J, Jacob ST, and Denny WA (2013) Structure-activity relationships for 4-anilinoquinoline derivatives as inhibitors of the DNA methyltransferase enzyme DNMT1. Bioorg. Med. Chem 21, 3147–3153. [PubMed: 23639684]

(44). McMahon JB, Currens MJ, Gulakowski RJ, Buckheit RW Jr., Lackman-Smith C, Hallock YF, and Boyd MR (1995) Michellamine B, a novel plant alkaloid, inhibits human immunodeficiency virus-induced cell killing by at least two distinct mechanisms. Antimicrob. Agents Chemother 39, 484–488. [PubMed: 7537029]

(45). Hobbs PD, Upender V, Liu JW, Pollart DJ, Thomas DW, and Dawson MI (1996) The first stereospecific synthesis of Michellamine B. Chem. Commun, 923–924.

(46). Augustus AM, Celaya T, Husain F, Humbard M, and Misra R (2004) Antibiotic-sensitive TolC mutants and their suppressors. J. Bacteriol 186, 1851–1860. [PubMed: 14996816]

(47). She W, Wang Q, Mordukhova EA, and Rybenkov VV (2007) MukEF is required for stable association of MukB with the chromosome. J. Bacteriol 189, 7062–7068. [PubMed: 17644586]

(48). Ge Q, Yamada Y, and Zgurskaya H (2009) The C-terminal domain of AcrA is essential for the assembly and function of the multidrug efflux pump AcrAB-TolC. J. Bacteriol 191, 4365–4371. [PubMed: 19411330]

(49). Zhan H, Swint-Kruse L, and Matthews KS (2006) Extrinsic interactions dominate helical propensity in coupled binding and folding of the lactose repressor protein hinge helix. Biochemistry 45, 5896–5906. [PubMed: 16669632]

(50). Petrushenko ZM, and Rybenkov VV (2017) Biochemical analysis of bacterial condensins. Methods Mol. Biol 1624, 145–159. [PubMed: 28842882]

(51). Kelley LA, Mezulis S, Yates CM, Wass MN, and Sternberg MJ (2015) The Phyre2 web portal for protein modeling, prediction and analysis. Nat. Protoc 10, 845–858. [PubMed: 25950237]

(52). Haynes KM, Abdali N, Jhawar V, Zgurskaya HI, Parks JM, Green AT, Baudry J, Rybenkov VV, Smith JC, and Walker JK (2017) Identification and structure-activity relationships of novel compounds that potentiate the activities of antibiotics in Escherichia coli. J. Med. Chem 60, 6205–6219. [PubMed: 28650638]

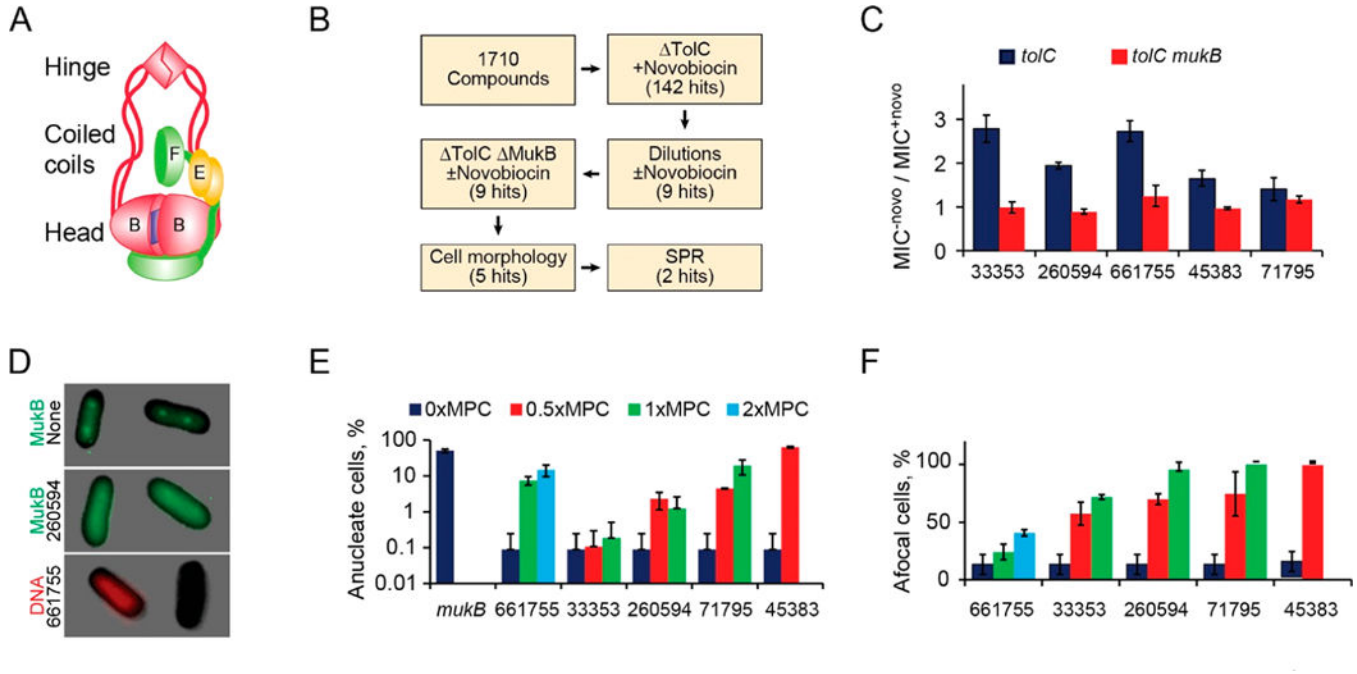


**Figure 1.**

(A) Architecture of the *E. coli* condensin MukBEF. The SMC subunit MukB dimerizes via the hinge and the ATP (blue square) mediated interface at the head. MukEF dynamically interacts with the head. (B) Flowchart of the screen. (C) Ratios of minimal inhibitory concentrations of the five hits in the presence or absence of 0.25× MIC of novobiocin for Δ*tolC* and Δ*tolC*Δ*mukB* cells (±SEM). (D) Examples of afocal and anucleate cells. MukB-GFP forms foci at 1/4 and 3/4 of the cell length in the absence (top) but not presence (middle) of a hit compound. Bottom panel shows Michellamine-induced formation of anucleate cells. (E, F) Frequency of anucleate (E) and afocal (F) cells at the indicated levels of the hit compounds, expressed as a fraction of the minimal potentiation concentration, MPC ($n > 100$; ±SD).

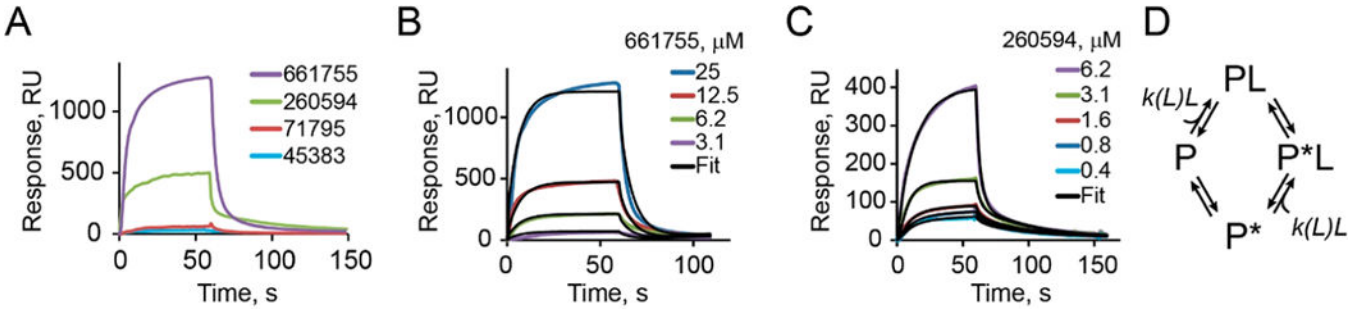


**Figure 2.**

SPR analysis of compound binding to MukB. (A) Sensograms of compound binding and dissociation for the indicated hit compounds injected at 25 μM. (B, C) SPR sensograms for Michellamine B (B) and 260594 (C) injected at the indicated concentrations. The data were globally fit to the model illustrated in panel D. (D) The compound binding model postulates a random order sequential conformational change and ligand binding. The rate of ligand binding was fit locally. The best fit binding rate increased with the concentration of the ligand, which indicates cooperative interactions.

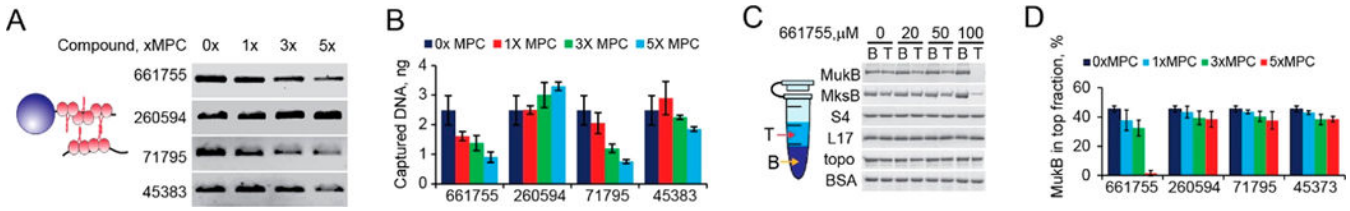


**Figure 3.**

Inhibition of MukB *in vitro*. (A) Inhibition of MukB-mediated DNA bridging. MukB is bound to a bead-tethered DNA, and another DNA is then added to be captured and recovered by MukB in the presence of the indicated amounts of the hit compounds. (B) The amount of MukB-captured DNA in the presence of the indicated compounds ($n \geq 2$, ±SD). (C) Michellamine-induced protein aggregation. Following 10 min of incubation, the aggregated protein was precipitated by low speed centrifugation, and the top and bottom fractions resolved by gel electrophoresis. (D) Percent of unaggregated MukB found in the top fraction after incubation with the indicated compounds ($n \geq 2$, ±SD).

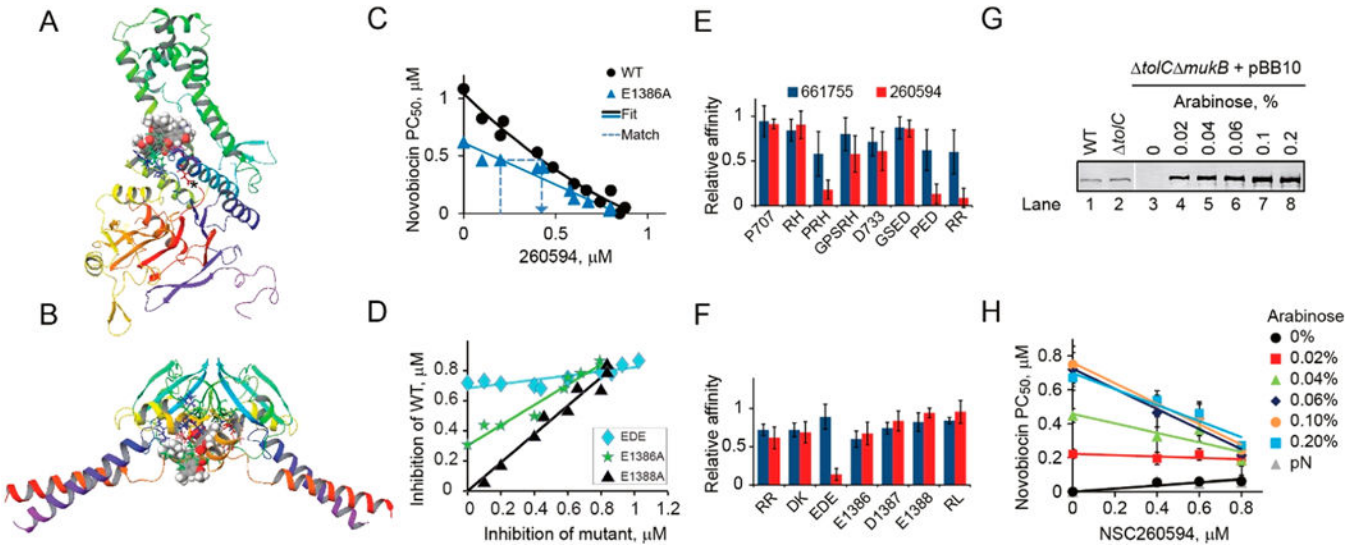


**Figure 4.**

Binding sites of Michellamine B and 260594. (A, B) Predicted binding sites for Michellamine B and NSC260594 in the head (A) and hinge (B) domains. Compounds are shown in spheres; side chains are shown for residues in the binding sites. (C) Effect of NSC260594 on novobiocin susceptibility of cells with the wild type and a mutant MukB. Potentiation concentration $PC_{50}$ of novobiocin was measured in the presence of the indicated amounts of the hit compound. The mutant and wild type data series were then matched by finding pairs of NSC260594 concentrations that produced the same novobiocin susceptibility in the two data sets and analyzed as illustrated in panel D. (D) NSC260594 inhibition curves for three representative mutants of MukB. The matching compound concentrations found as in panel C were plotted against each other and fit to a straight line. The slope of the fit line provides the upper bound on the ratio of the compound affinities to the mutant and wild type MukB. (E, F) Relative affinities of the hinge (E) and head (F) domain MukB mutants to the indicated hit compounds. (G) Immunoblotting analysis of MukB expression in BW25113 (WT), ETBW (Δ*tolC*), and OU142 (Δ*tolC* Δ*mukB*) cells harboring MukB-producing pBB10 plasmid. Lanes 1−3 and 4−10 contain extract form 0.1 and 0.004 OD of cells, respectively. MukB was detected using anti-MukB antibody.[26] (H) Dose-dependent susceptibility of MukB overproducing OU142 cells harboring pBB10 plasmid to NSC260594, measured as the potentiation concentration of novobiocin in the presence of the indicated amounts of the compound and arabinose. pN, empty plasmid.

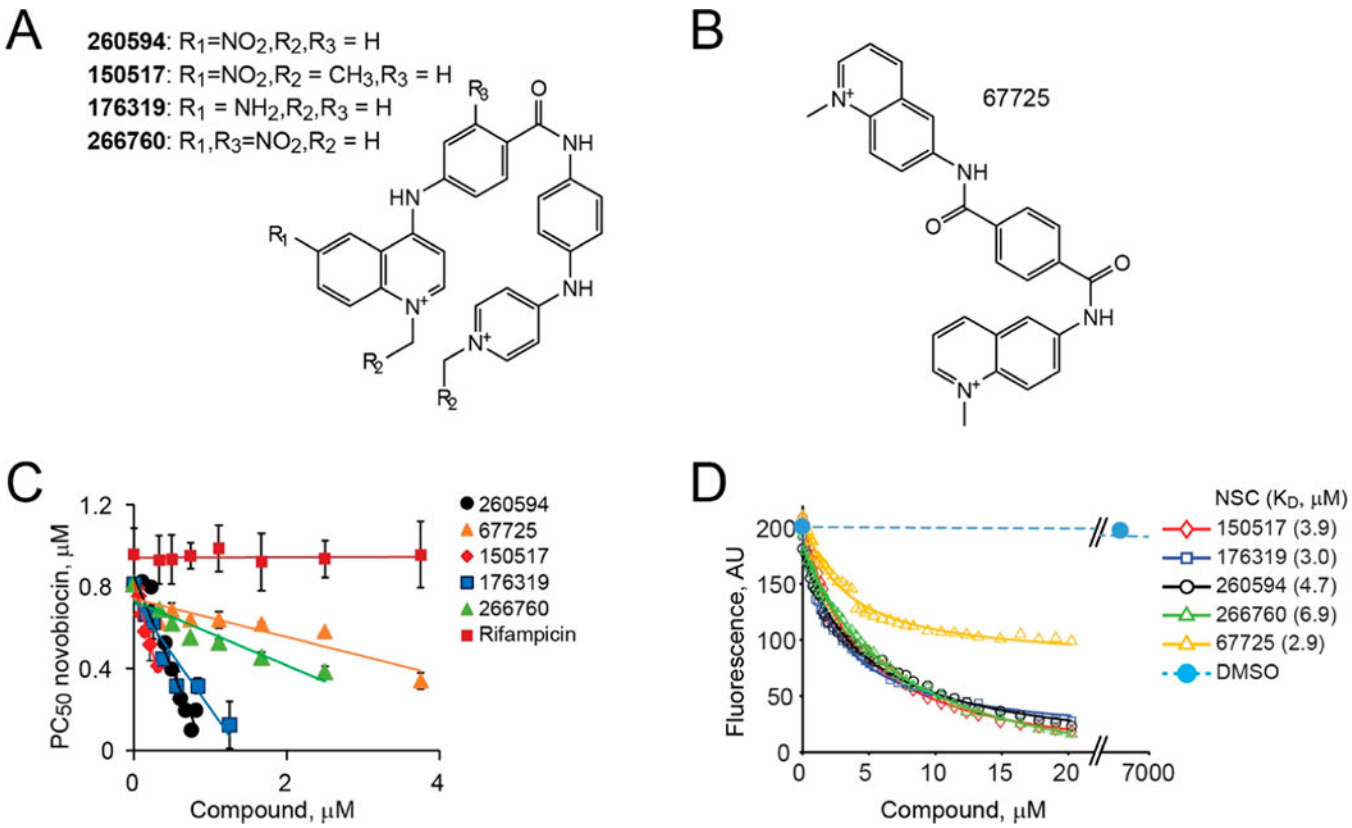


**Figure 5.**

Structure activity relationship among analogs of NSC260594. (A) Chemical structures of the tested NSC260594 analogs. (B) Chemical structure of NSC67725. (C) Potentiation concentrations of novobiocin in the presence of the indicated amounts of the compound. (D) Tryptophan fluorescence of MukB in the presence of the indicated amounts of the compounds.

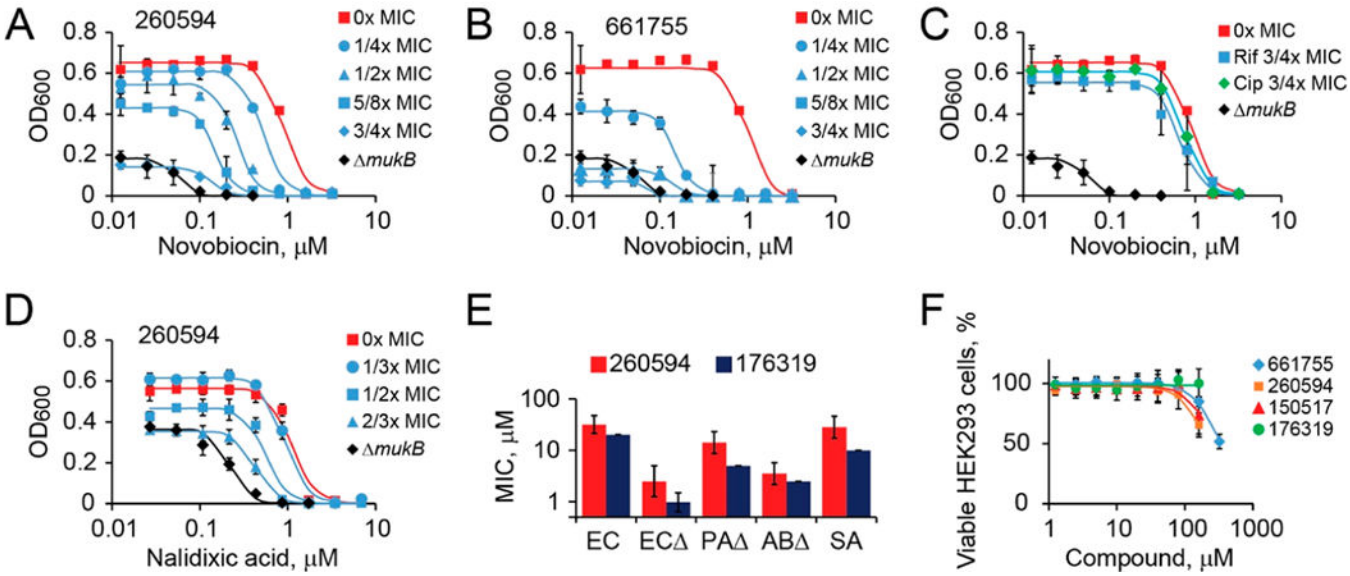


**Figure 6.**

Potentiation activity of condensin inhibitors. (A−C) Novobiocin potentiation by the indicated concentrations of NSC260594 (A), Michellamine B (B), and rifampicin or ciprofloxacin (C) in Δ*tolC* or Δ*tolC*Δ*mukB E. coli* in LB at 37 °C. (D) Potentiation of nalidixic acid by NSC260594 in Δ*tolC E. coli*. (E) MIC of NSC176319 and NSC260594 (±SD) in *E. coli* BW25115 (EC) and Δ*tolC* ETBW (ECΔ), P. *aeruginosa* GKCW122 (PAΔ), *Acinetobacter baumannii* IL123 (ABΔ), and *Staphylococcus aureus* (SA). (F) Viability of HEK293 cells in the presence of condensin inhibitors.